

N 70 24384

**NASA TECHNICAL
MEMORANDUM
NASA TM X-53990**

**TORSIONAL VIBRATION ANALYSIS
OF SATURN VEHICLES**

By Larry Kiefling and Frank Bugg
Aero-Astroynamics Laboratory

February 27, 1970

**CASE FILE
COPY**

NASA

*George C. Marshall Space Flight Center
Marshall Space Flight Center, Alabama*

1. REPORT NO. TM X-53990		2. GOVERNMENT ACCESSION NO.		3. RECIPIENT'S CATALOG NO.	
4. TITLE AND SUBTITLE Torsional Vibration Analysis of Saturn Vehicles				5. REPORT DATE February 27, 1970	
				6. PERFORMING ORGANIZATION CODE	
7. AUTHOR(S) Larry Kiefling and Frank Bugg				8. PERFORMING ORGANIZATION REPORT #	
9. PERFORMING ORGANIZATION NAME AND ADDRESS George C. Marshall Space Flight Center Marshall Space Flight Center, Alabama 35812				10. WORK UNIT NO.	
				11. CONTRACT OR GRANT NO.	
				13. TYPE OF REPORT & PERIOD COVERED Technical Memorandum	
12. SPONSORING AGENCY NAME AND ADDRESS				14. SPONSORING AGENCY CODE	
15. SUPPLEMENTARY NOTES Prepared by Aero-Astroynamics Laboratory, Science and Engineering Directorate					
16. ABSTRACT <p>Methods for finding the torsional vibration modes for either a beam-like vehicle, such as Saturn V, or a multibeam vehicle, such as Saturn IB, are developed. The single beam analysis is a Stodola iteration method. The Saturn IB vehicle is mathematically modeled as a system of beams and connecting members. The modes of the vehicle are composed of the superimposed components of normal beam modes plus rigid body motion.</p> <p>A comparison is made with dynamic test data. The calculated frequencies differed from the experimental values by an average of 8 percent for the cases compared.</p>					
17. KEY WORDS			18. DISTRIBUTION STATEMENT Public Release <i>C. D. Egan</i>		
19. SECURITY CLASSIF. (of this report) Unclassified		20. SECURITY CLASSIF. (of this page) Unclassified		21. NO. OF PAGES 36	22. PRICE \$ 3. 00

TABLE OF CONTENTS

	Page
SUMMARY	1
INTRODUCTION	1
ANALYSIS	2
Single-Beam Analysis	2
Multiple Beam Analysis	7
COMPARISON WITH EXPERIMENT	15
REFERENCES	27

LIST OF ILLUSTRATIONS

Figure	Title	Page
1.	Schematic of Saturn IB mathematical model	18
2.	First outer tank mode at lift-off	19
3.	First torsional mode at lift-off	20
4.	Command module mode at lift-off	21
5.	Command module with center body mode at lift-off	22
6.	Second outer tank mode at lift-off	23
7.	First torsional mode at cut-off	24
8.	Command module mode at cut-off	25
9.	Saturn IB SA-202 Configuration	26

LIST OF TABLES

Table	Title	Page
1.	FREQUENCY AND GENERALIZED MASS ACCURACY (tolerance = 0.001).	17
2.	FREQUENCY AND GENERALIZED MASS ACCURACY (tolerance = 0.0001)	17

DEFINITION OF SYMBOLS

D	Column matrix of $r_{a1}^{\theta_{a1}}, r_{a2}^{\theta_{a2}}, r_{a3}^{\theta_{a3}}$
$J_{a1}, J_{a2}, J_{a3}, J_b$	Rigid body inertia values for $\theta_{a1}, \theta_{a2}, \theta_{a3}$, and θ_b degrees of freedom, respectively.
J_{ui}, J_{cj}	Modal generalized inertias for upper stages and center tank, respectively.
J'_u, J'_c	Mass moment of inertia per unit length for upper stages and center tank, respectively.
K	Spider beam stiffness matrix
K_c	Center tank torsion spring constant, calculated in single-beam program.
K_{ab}	Outer tank torsional spring constant
K_{at}, K_{bt}	Rotational spring constants restraining tangential slope of outer tank top and bottom, respectively.
K_s	Suspension spring constant
l_u, l_c, l_t	Length of upper stages, center tank, and outer tanks, respectively
m'_t	Modal generalized mass for outer tank
r_{a1}, r_{a2}, r_{a3}	Radial distances to center tank, outer tank, and upper stage attach points, respectively, on spider beam.

DEFINITION OF SYMBOLS (Continued)

R	Radial distance to outer tanks
x	Longitudinal coordinate
x_a, x_b	Coordinate at top and bottom of outer tanks, respectively
y_{tk}	Modal bending displacement for outer tanks
y_{atk}, y_{btk}	Modal slope of outer tank at top and bottom, respectively
θ_{a1}	Spider beam rotation at booster center tank attach point
θ_{a2}	Spider beam rotation at booster outer tank attach point
θ_{a3}	Spider beam rotation at upper stage attach point
θ_b	Booster thrust structure rotation
θ_{ui}	Modal rotational displacement of upper stages
θ_{cj}	Modal rotational displacement of center tank
λ_{tk}	Outer tank tangential bending modal amplitudes, t is tank number, k is mode number, n_t modes
τ_{ui}	Upper stage modal amplitude, n_u modes
τ_{cj}	Booster center tank modal amplitude, n_c modes

DEFINITION OF SYMBOLS (Concluded)

$\omega_{ui}, \omega_{cj}, \omega_{tk}$	Modal natural frequencies (radians per second) of upper stages, center tank and outer tanks, respectively
$T_{\mu}^{(n)}$	Torque distribution, mode number μ and iteration number n
c	First station on missile
d	Last station on missile
$GJ(x)$	Torsional stiffness values

TORSIONAL VIBRATION ANALYSIS OF SATURN VEHICLES

SUMMARY

Methods for finding the torsional vibration modes for either a beam-like vehicle, such as Saturn V, or a multibeam vehicle, such as Saturn IB, are developed. The single beam analysis is a Stodola iteration method. The Saturn IB vehicle is mathematically modeled as a system of beams and connecting members. The modes of the vehicle are composed of the superimposed components of normal beam modes plus rigid body motion.

A comparison is made with dynamic test data. The calculated frequencies differed from the experimental values by an average of 8 percent for the cases compared.

INTRODUCTION

This program was developed to find the normal torsional vibration modes (frequencies and mode shapes) of space vehicles, especially Saturn IB vehicles.

Torsional vibration modes of the Saturn IB and other clustered booster-type vehicles cannot, of course, be analyzed by the usual beam type of analysis. While it is possible to write a general matrix solution to the total vehicle represented as a lumped-mass system and solve for all modes, this method is usually not practical for large structures because of computational problems. The superimposed normal mode technique used here has been found to give accurate results for the lower modes of the vehicle. A similar method for bending vibrations is described in Reference 1. A proof of the independence of the bending and torsional modes is given in Reference 2.

In the idealized model, the beams on the vehicle centerline are vibrating in torsion while the booster outer tanks are bending tangentially. The torsional modes for the center beams are calculated within the program; the bending modes are calculated by the Stodola bending program [3] and the data are transferred on magnetic tape. The beam torsion portion of the program is also used alone to analyze single-beam vehicles, such as the Saturn V.

ANALYSIS

This program is divided into two parts. The first part analyzes any vehicle that can be represented by a beam, and the second specifically analyzes the Saturn IB vehicles.

Modes for vehicles that can be represented by a beam are calculated by a Stodola iteration technique. Options exist for the three possible end conditions: free-free, cantilever, and clamped-clamped. A special feature is a data-interpolation routine to convert data from furnished stations and units to the system desired for use in the program.

The second or multibeam part of the program is specifically for analysis of Saturn IB torsional vibrations. Torsion modes of the upper stage and center tank, tangential bending modes of the outer tanks, and rotations of the rigid masses provide the degrees of freedom for the system. Certain modes that involve outer tank motion only and that are of no interest are lost in grouping the four outer tanks of each type. Expressions for kinetic and potential energy are used to derive a matrix equation by use of Lagrange's equation. The matrix equation is solved for eigenvalues to find the vehicle mode shapes.

Single-Beam Analysis

The Stodola method for beam torsional vibrations is an iterative integration method. Basically, a torque distribution, which is integrated to find the deflections at each station, is assumed, and a new torque distribution is calculated from the inertial loading. The iteration is repeated until the frequency, as calculated from energy considerations, converges within the desired tolerance. Provision is made for all end conditions. The geometry of the model is given in Figure 1.

First, an initial torque distribution is assumed:

free-free

$$T_{\mu}^{(0)}(x) = (x-c)(x-d) \prod_{\nu=1}^{\nu=\mu-1} \left[x-c-\frac{\nu}{\mu}(d-c) \right], \quad (1a)$$

cantilever

$$T_{\mu}^{(0)}(x) = (x-d)^2 \prod_{\nu=1}^{\nu=\mu-1} \left[x-c - \frac{\nu}{\mu} (d-c) \right] , \quad (1b)$$

clamped-clamped

$$T_{\mu}^{(0)}(x) = \prod_{\nu=1}^{\nu=\mu} \left[x-c - \frac{\nu}{\mu+1} (d-c) \right] \quad (1c)$$

The subscript μ always denotes the mode number, while the superscript in parenthesis denotes the iteration number.

Next, the torsional displacements are calculated:

$$\bar{\theta}_{\mu}^{(n)}(x) = \int_c^x \frac{T_{\mu}^{(n-1)}(x)}{GJ(x)} dx , \quad (2)$$

free-free

$$\theta_{0\mu}^{(n)} = - \frac{\int_c^d J' \bar{\theta}_{\mu}^{(n)}(x) dx}{J} , \quad (3a)$$

cantilever, clamped-clamped

$$\theta_{0\mu}^{(n)} = 0 \quad (3b, 3c)$$

$$\theta_{\mu}^{(n)*}(x) = \bar{\theta}_{\mu}^{(n)}(x) + \theta_{0\mu_1}^{(n)} \quad (4)$$

For modes other than the first, the mode shapes must be purified by removing components of all lower modes.

$$a_{\nu}^{(n)} = \frac{\int_c^d J' \theta_{\nu}^{(n)}(x) dx}{\int_c^d J' \theta_{\nu}^2(x) dx} \quad (5)$$

$$\tilde{\theta}_{\mu}^{(n)}(x) = \theta_{\mu}^{(n)*}(x) - \sum_{\nu=1}^{\nu=\mu-1} a_{\nu}^{(n)} \theta_{\nu 1} \quad (6)$$

The square of the circular frequency can now be calculated from energy considerations.

$$\omega_{\mu}^{(n)2} = \frac{\int_c^d \frac{T_{\mu}^{(n-1)2}(x)}{GJ(x)} dx}{\int_c^d J' \tilde{\theta}_{\mu}^{(n)2}(x) dx} \quad (7)$$

The mode is then normalized by dividing by the displacement with the largest absolute value:

$$\theta_{\mu}^{(n)}(x) = \frac{\tilde{\theta}_{\mu}^{(n)}(x)}{\tilde{\theta}_{\mu 1}^{(n)}(x)} \quad (8)$$

The torque caused by inertial loading can now be calculated and the boundary conditions applied.

$$T_{\mu}^{(n)}(x) = \int_c^x J' \theta_{\mu}^{(n)}(x) dx + T_{o\mu}^{(n)} \quad , \quad (9)$$

free-free

$$T_{o\mu}^{(n)} = 0 \quad , \quad (10a)$$

cantilever

$$T_{o\mu}^{(n)} = - \int_c^d J' \theta_{\mu}^{(n)}(x) dx \quad , \quad (10b)$$

clamped-clamped

$$T_{o\mu}^{(n)} = - \int_{c+\Delta x}^{d-\Delta x} \left\{ J \theta_{\mu}^{(n)}(x) \frac{\left(\frac{1}{x-c}\right)^2}{\left(\frac{1}{d-x}\right)^2 \left[\frac{\int_c^d GJ(x) dx}{\int_c^x GJ(x) dx} - 1 \right]} \right\} dx \quad 10c$$

A test for convergence can now be made.

If

$$\left| \frac{\omega_{\mu}^{(n-1)^2}}{\omega_{\mu}^{(n)^2}} - 1 \right| < \delta \quad , \quad (11)$$

the program has converged. The final values of $\theta_{\mu}^{(n)}(x)$, $T_{\mu}^{(n)}(x)$ and $\omega_{\mu}^{(n)^2}$ will be designated $\theta_{\mu}(x)$, $T_{\mu}(x)$ and ω_{μ}^2 , respectively.

If the program has not converged, $T_{\mu}^{(n)}(x)$ from equation (9) is entered as $T_{\mu}^{(n-1)}(x)$ in equation (2), and the iteration is repeated. Several terms of interest may be calculated after the last iteration.

$$f_{\mu} = \frac{\omega_{\mu}}{2\Pi} \quad (12)$$

$$J_{\mu} = \int_c^d J'(x) \theta_{\mu}^2(x) dx \quad (13a)$$

$$V_{\mu} = \omega_{\mu}^2 J_{\mu} \quad (13b)$$

$$J = \int_c^d J'(x) dx \quad (14)$$

$$H_{\mu} = \int_c^d J'(x) \theta_{\mu}(x) dx \quad (15)$$

The following are calculated only for clamped-clamped beams:

$$J_{1c} = \int_c^d J'(x) \left(\frac{x-c}{d-c} \right) dx \quad (16)$$

$$J_{2c} = \int_c^d J'(x) \left(\frac{x-c}{d-c} \right)^2 dx \quad (17)$$

$$N_{c\mu} = \int_c^d J'(x) \left(\frac{x-c}{d-c} \right) \theta_{\mu}(x) dx \quad (18)$$

$$k_c = \frac{1}{\int_c^d \frac{1}{GJ(x)} dx} \quad (19)$$

A uniform beam was analyzed and comparisons were made between exact solution results and Stodola method results in Tables 1 and 2 for $\delta=0.001$ and $\delta=0.0001$, respectively. Decreasing the tolerance from 0.001 to 0.0001 had little effect on the frequency prediction accuracy, but the accuracy of the generalized mass calculations was improved.

Multiple Beam Analysis

The Saturn IB vehicle is idealized as a system of beams connected by elastic and rigid members. A schematic view of the model is shown in Figure 1. The upper stages are modeled as a torsional beam cantilevered from the top of the spider beam, and the center tank is modeled as a clamped-clamped torsional beam. The outer tanks of the booster are given degrees of freedom bending tangentially. Because of the symmetry, the four tanks of each kind (LOX and fuel) can be lumped into one beam of each kind. The outer tanks have a hinge with a rotational spring at each end. The tail structure is considered to be rigid. The spider beam has degrees of freedom defined for the rigid-ring attach points of the center tank, outer tanks, and upper stages.

The motion of the vehicle is defined in terms of the linear and angular displacements defined above and in Figure 1. The kinetic energy (KE) and potential energy (PE) can be expressed as follows:

$$\begin{aligned}
 \text{KE} = & \frac{1}{2} \int_{1\mu} J'_{\mu}(x) \left[\dot{\theta}_{a3} + \sum_{i=1}^n \dot{\tau}_{\mu i} \theta_{\mu i}(x) \right]^2 dx \\
 & + \frac{1}{2} \int_{1c} J'_{c}(x) \left[\dot{\theta}_b + \frac{x-x_b}{x_a-x_b} (\dot{\theta}_{a1} - \dot{\theta}_b) + \sum_{j=1}^{nc} \dot{\tau}_{cj} \theta_{cj}(x) \right]^2 dx \\
 & + 4 \sum_{t=1}^2 \frac{1}{2} \int_{1t} R^2 m'_t(x) \left[\dot{\theta}_b + \frac{x-x_b}{x_a-x_b} (\dot{\theta}_{a2} - \dot{\theta}_b) \right. \\
 & \quad \left. + \frac{1}{R} \sum_{k=1}^{nt} \dot{\lambda}_{tk} y_{tk}(x) \right]^2 dx \\
 & + \frac{1}{2} J_{a1} \dot{\theta}_{a1}^2 + \frac{1}{2} J_{a2} \dot{\theta}_{a2}^2 + \frac{1}{2} J_{a3} \dot{\theta}_{a3}^2 + \frac{1}{2} J_b \dot{\theta}_b^2
 \end{aligned}$$

$$\begin{aligned}
PE &= \frac{1}{2} \sum_{i=1}^{n\mu} \tau_{\mu i}^2 \omega_{\mu i}^2 J_{\mu i} + \frac{1}{2} \sum_{j=1}^{nc} \tau_{c j}^2 \omega_{c j}^2 J_{c j} \\
&+ \frac{1}{2} \sum_{t=1}^2 \sum_{K=1}^{nt} \lambda_{tk}^2 \omega_{tk}^2 M_{tk} + \frac{1}{2} K_c \left(\theta_{a1} - \theta_b \right)^2 + \frac{1}{2} K_{ab} \left(\theta_{a2} - \theta_b \right)^2 \\
&+ \sum_{t=1}^2 \frac{1}{2} K_{at} \left(R \frac{\theta_{a2} - \theta_b}{x_a - x_b} + \sum_{k=1}^{nt} \lambda_{tk} y'_{atk} \right)^2 \\
&+ \sum_{t=1}^2 \frac{1}{2} K_{bt} \left(R \frac{\theta_{a2} - \theta_b}{x_a - x_b} + \sum_{k=1}^{nt} \lambda_{tk} y'_{btk} \right)^2 \\
&+ \frac{1}{2} D_t K D + \frac{1}{2} k_s \theta_b^2 \quad .
\end{aligned}$$

Lagrange's equation, $\frac{d}{dt} \left(\frac{\delta KE}{\delta \dot{q}_i} \right) + \frac{\delta PE}{\delta q} = 0$, is applied to obtain

the resulting matrix equation, $([A] - \omega^2 [B]) \{q\} = 0$.

A MATRIX

$$A_{11} = r_{a1}^2 K_{11} + K_c$$

$$A_{12} = r_{a1} r_{a2} K_{12}$$

$$A_{13} = r_{a1} r_{a3} K_{13} \quad , \quad A_{14} = -K_c$$

$$A_{1i} = A_{1j} = A_{1k} = 0$$

$$A_{21} = r_{a2} r_{a1} K_{21}$$

$$A_{22} = \frac{R^2}{l^2} \sum_{t=1}^2 (K_{at} + K_{bt}) + r_{a2}^2 K_{22} + k_{ab}$$

$$A_{23} = r_{a2} r_{a3} K_{23}$$

$$A_{24} = - \left[\frac{R^2}{l^2} \sum_{t=1}^2 (K_{at} + K_{bt}) + K_{ab} \right]$$

$$A_{2i} = A_{2j} = 0$$

$$A_{2tk} = \frac{R}{l} (K_{at} y'_{atk} + K_{bt} y'_{btk})$$

$$A_{31} = r_{a3} r_{a1} K_{31}$$

$$A_{32} = r_{a3} r_{a2} K_{32}$$

$$A_{33} = r_{a3}^2 K_{33}$$

$$A_{3i} = A_{3j} = A_{3k} = 0 = A_{34}$$

$$A_{41} = 0$$

$$A_{42} = - \left[\frac{R^2}{l^2} \sum_{t=1}^2 (K_{at} + K_{bt}) + K_{ab} \right]$$

$$A_{43} = 0$$

$$A_{44} = \frac{R^2}{l^2} \sum_{t=1}^2 (K_{at} + K_{bt}) + K_c + K_s + K_{ab}$$

$$A_{4i} = A_{4j} = 0$$

$$A_{4tk} = - \frac{R}{l} (K_{at} y'_{atk} + K_{bt} y'_{btk})$$

$$A_{i1} = A_{i2} = A_{i3} = A_{i4} = 0$$

$$A_{i\underline{i}} = \omega_{ui}^2 J_{ui} \quad \text{for } i = \underline{i}, \quad A_{i\underline{i}} = 0 \quad \text{for } i \neq \underline{i}$$

$$A_{i\underline{j}} = A_{i\underline{tk}} = 0$$

$$A_{j1} = A_{j2} = A_{j3} = A_{j4} = 0$$

$$A_{\underline{j}i} = 0$$

$$A_{\underline{j}\underline{j}} = \omega_{cj}^2 J_{cj} \quad \text{for } j = \underline{j}, \quad A_{\underline{j}\underline{j}} = 0 \quad \text{for } j \neq \underline{j}$$

$$A_{\underline{j}k} = 0$$

$$A_{tk1} = 0$$

$$A_{tk2} = \frac{R}{I} (K_{at} y'_{atk} + K_{bt} y'_{btk})$$

$$A_{tk3} = 0$$

$$A_{tk4} = -\frac{R}{I} (K_{at} y'_{atk} + K_{bt} y'_{btk})$$

$$A_{tki} = A_{tkj} = 0$$

$$A_{tk, \underline{tk}} = \sum_{\underline{k}=1}^{nt} (K_{at} y'_{atk} y'_{atk} + K_{bt} y'_{btk} y'_{btk}) + \omega_{tk}^2 M_{tk} \quad \text{for } k = \underline{k}$$

B MATRIX

$$B_{11} = J_{1c} + J_{a1}$$

$$B_{12} = B_{13} = 0$$

$$B_{14} = J_{1c} - J_{2c}$$

$$B_{\underline{1i}} = 0$$

$$B_{\underline{1j}} = N_{cj}$$

$$B_{1\underline{tk}} = 0$$

$$B_{21} = 0$$

$$B_{22} = 4 \frac{R^2}{I^2} \sum_{t=1}^2 \left[(N_{ot} - 2x B_t M_{ot} + x B_t^2 m_t) + J_{a2} \right]$$

$$B_{23} = 0$$

$$B_{24} = 4 \frac{R^2}{I} \sum_{t=1}^2 \left[M_{ot} - x B_t m_t - \frac{1}{I} (N_{ot} - 2x B_t M_{ot} + x B_t^2 m_t) \right]$$

$$B_{2\underline{i}} = B_{2\underline{j}} = 0$$

$$B_{2\underline{tk}} = 4 \frac{R}{I} \left[J T_{tk} + (xMC_t - xB_t) HT_{tk} \right]$$

$$B_{31} = B_{32} = 0$$

$$B_{33} = J_u + J_{a3}$$

$$B_{34} = 0$$

$$B_{3\underline{i}} = H_{ui}$$

$$B_{3\underline{j}} = B_{3\underline{tk}} = 0$$

$$B_{41} = J_{1c} - J_{2c}$$

$$B_{42} = 4 \frac{R^2}{l^2} \sum_{t=1}^2 \left[-N_{ot} + (2xB_t + 1) M_{ot} - (xB_t^2 + lxB_t) m_t \right]$$

$$B_{43} = 0$$

$$B_{44} = 4 \frac{R^2}{l^2} \sum_{t=1}^2 \left[N_{ot} - 2(1 + xB_t) M_{ot} + (l^2 + 2lxB_t + xB_t^2) m_t \right] \\ + J_{oc} - 2J_{1c} + J_{2c} + J_b$$

$$B_{\underline{4i}} = 0$$

$$B_{4j} = H_{cj} - N_{cj}$$

$$B_{4t\underline{k}} = 4 \frac{R}{l} \left[(1 - xmc_t + xB_t) HT_{t\underline{k}} - JT_{t\underline{k}} \right]$$

$$B_{i1} = B_{i2} = 0$$

$$B_{i3} = H_{ui}$$

$$B_{i4} = 0$$

$$B_{\underline{ii}} = J_{ui} \quad \text{for } i = \underline{i} \quad , \quad B_{\underline{ii}} = 0 \quad \text{for } i \neq \underline{i}$$

$$B_{\underline{j}\underline{j}} = B_{\underline{i}\underline{t}\underline{k}} = 0$$

$$B_{\underline{j}\underline{1}} = N_{\underline{c}\underline{j}}$$

$$B_{\underline{j}\underline{2}} = B_{\underline{j}\underline{3}} = 0$$

$$B_{\underline{j}\underline{4}} = H_{\underline{c}\underline{j}} - N_{\underline{c}\underline{j}}$$

$$B_{\underline{j}\underline{i}} = 0$$

$$B_{\underline{j}\underline{j}} = J_{\underline{c}\underline{j}} \quad \text{for } j = \underline{j} \quad , \quad B_{\underline{j}\underline{i}} = 0 \quad \text{for } j \neq \underline{j}$$

$$B_{\underline{j}\underline{t}\underline{k}} = 0$$

$$B_{\underline{t}\underline{k}\underline{1}} = 0$$

$$B_{\underline{t}\underline{k}\underline{2}} = 4 \frac{R}{l} \left[J T_{\underline{t}\underline{k}} + (x m c_{\underline{t}} - x B_{\underline{t}}) H T_{\underline{t}\underline{k}} \right]$$

$$B_{\underline{t}\underline{k}\underline{3}} = 0$$

$$B_{\underline{t}\underline{k}\underline{4}} = 4 \frac{R}{l} \left[-J T_{\underline{t}\underline{k}} + (1 - x m c_{\underline{t}} + x B_{\underline{t}}) H_{\underline{t}\underline{k}} \right]$$

$$B_{\underline{t}\underline{k}\underline{i}} = B_{\underline{t}\underline{k}\underline{j}} = 0$$

$$B_{\underline{t}\underline{k}, \underline{t}\underline{k}} = M_{\underline{t}\underline{k}} \quad \text{for } k = \underline{k} \quad , \quad B_{\underline{t}\underline{k}, \underline{t}\underline{k}} = 0 \quad \text{for } k \neq \underline{k} \quad ,$$

where

J_{1c} , J_{2c} , N_{cj} , J_u , H_{ui} , H_{cj} , J_{ui} , and J_{cj} are as defined for the single-beam analysis with subscripts "u" and "c" designating upper stage and center tank, respectively, and "i" and "j" are modal indexes.

$$N_{ot} = \int_1 x^2 m'(x) dx$$

xMc_t = mass center for outer tank.

$$M_{ot} = \int_1 xm'(x) dx$$

$$m_t = \int_1 m'(x) dx$$

$$JT_{tk} = \int_1 m'(x) \bar{x} y_{tk}(x) dx$$

$$HT_{tk} = \int_1 m'(x) y_{tk}(x) dx$$

xB_t = outer tank lower end coordinate.

COMPARISON WITH EXPERIMENT

Mode shapes and frequencies calculated by the multibeam torsion program are compared with experimentally determined modes in Figures 2 through 8. The experimental data were taken from References 4 and 5, which report dynamic tests of a Saturn IB type launch vehicle. The particular data compared are for the test vehicle in the SA-202 configuration (Fig. 9) and for mass distributions corresponding to the conditions at lift-off and at first stage cut-off.

In the dynamic tests two of the first stage oxygen tanks and two fuel tanks were instrumented. The dynamic tests, therefore, showed some of the modes involving motion of one oxygen tank relative to the other and the fuel tanks relative to each other. These modes are not defined by the program since the mathematical model used only three beams to represent the first stage; one beam represented the four outer LOX tanks, one represented the four fuel tanks, and one represented the center tank. The first four calculated modes corresponded to the first four experimental modes (Fig. 2 through 5). Two of the modes involving relative motion of first stage oxygen and fuel tanks were found in the dynamic tests at frequencies between those in Figures 5 and 6. For the modes and frequencies presented, the calculated frequencies differed from the measured frequencies by an average of 8 percent.

TABLE 1. FREQUENCY AND GENERALIZED MASS ACCURACY
(tolerance = 0.001)

End Cond.	Mode	ω Exact	ω Stodola	Percent Error	G. Mass Exact	G. Mass Stodola	Percent Error
Canti-lever	1	0.01283	0.01283	0.00	150.00	150.05	0.03
	2	0.03848	0.03848	0.00	150.00	149.33	0.44
	3	0.06413	0.06417	0.06	150.00	147.66	1.56
	4	0.08977	0.08988	0.12	150.00	146.77	2.15
Free-free	1	0.02565	0.02565	0.00	150.00	149.95	0.03
	2	0.05130	0.05132	0.04	150.00	148.79	0.81
	3	0.07695	0.07701	0.07	150.00	148.06	1.29
	4	0.10260	0.10274	0.14	150.00	148.41	1.06
Clamped-clamped	1	0.02565	0.02565	0.00	150.00	150.13	0.09
	2	0.05130	0.05132	0.04	150.00	147.63	1.58
	3	0.07695	0.07701	0.07	150.00	146.78	2.15
	4	0.10260	0.10277	0.17	150.00	142.35	5.10

TABLE 2. FREQUENCY AND GENERALIZED MASS ACCURACY
(tolerance = 0.0001)

End Cond.	Mode	ω Exact	ω Stodola	Percent Error	G. Mass Exact	G. Mass Stodola	Percent Error
Canti-lever	1	0.01283	0.01283	0.00	150.00	150.05	0.03
	2	0.03848	0.03848	0.00	150.00	149.79	0.14
	3	0.06413	0.06416	0.05	150.00	149.51	0.33
	4	0.08977	0.08987	0.11	150.00	149.58	0.28
Free-free	1	0.02565	0.02565	0.00	150.00	149.95	0.03
	2	0.05130	0.05132	0.04	150.00	149.70	0.20
	3	0.07695	0.07701	0.07	150.00	149.34	0.44
	4	0.10260	0.10274	0.14	150.00	149.08	0.61
Clamped-clamped	1	0.02565	0.02565	0.00	150.00	150.01	0.01
	2	0.05130	0.05132	0.04	150.00	149.52	0.32
	3	0.07695	0.07701	0.07	150.00	149.38	0.41
	4	0.10260	0.10274	0.14	150.00	148.34	1.11

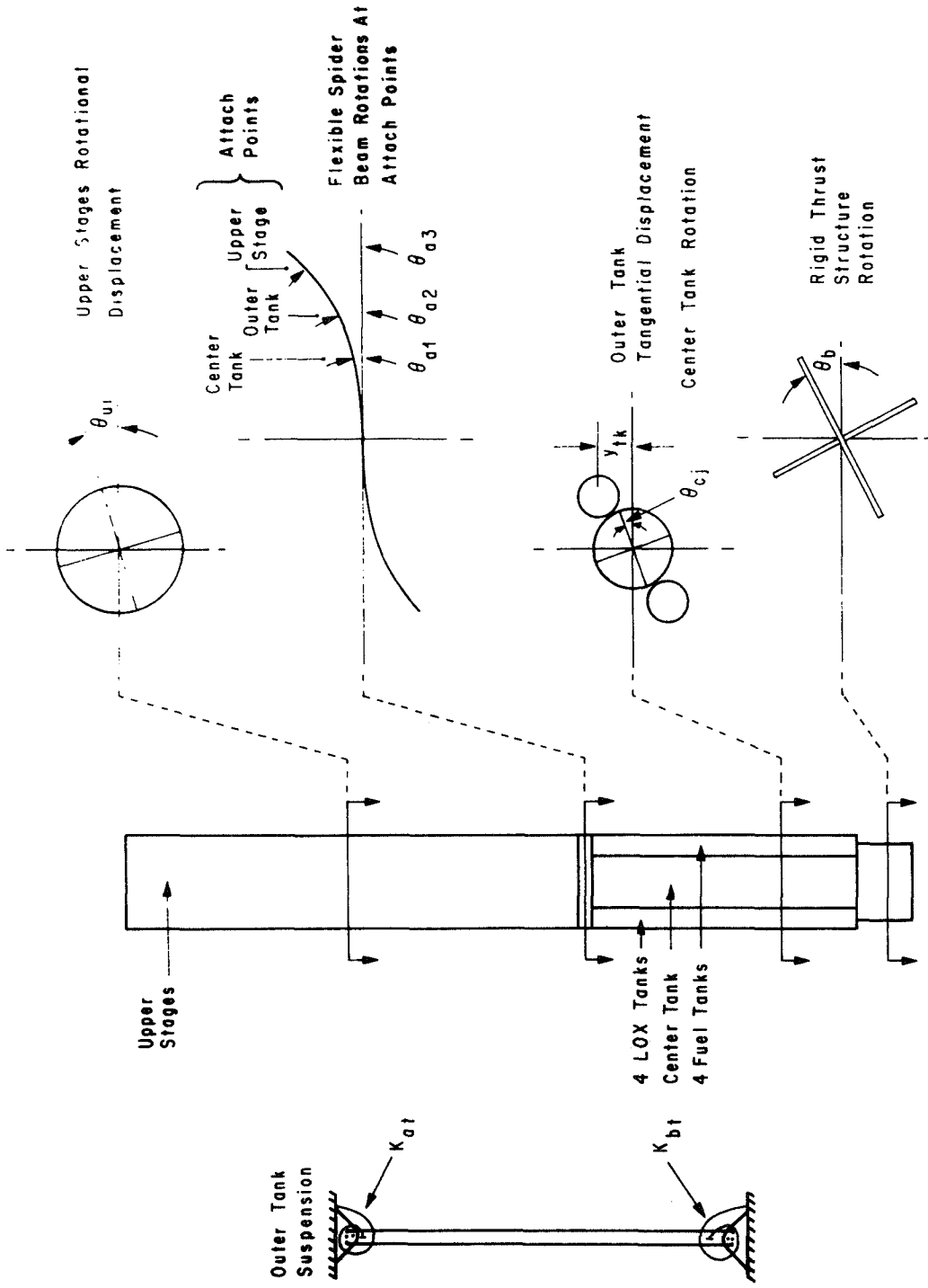


Figure 1. Schematic of Saturn IB mathematical model.

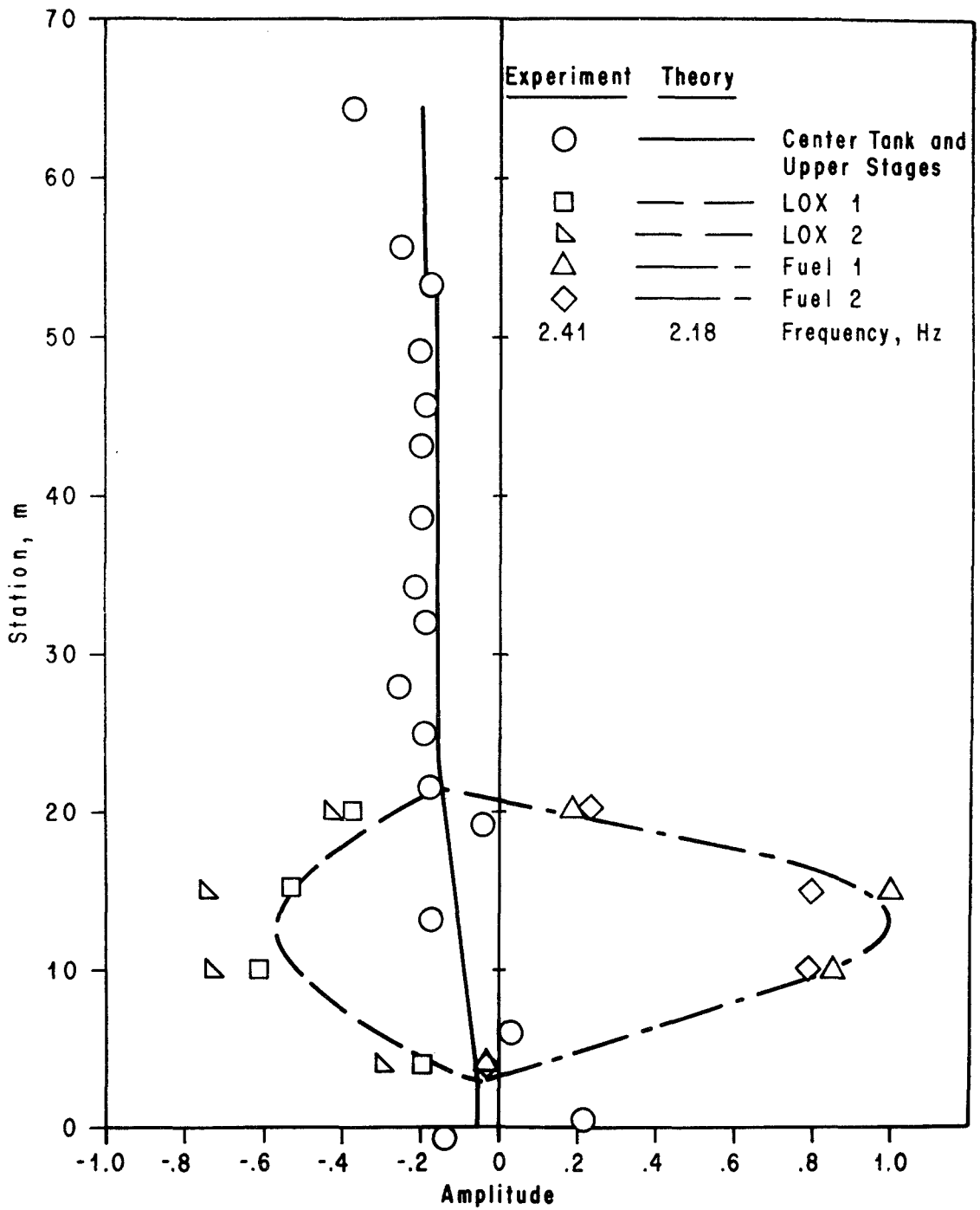


Figure 2. First outer tank mode at lift-off.

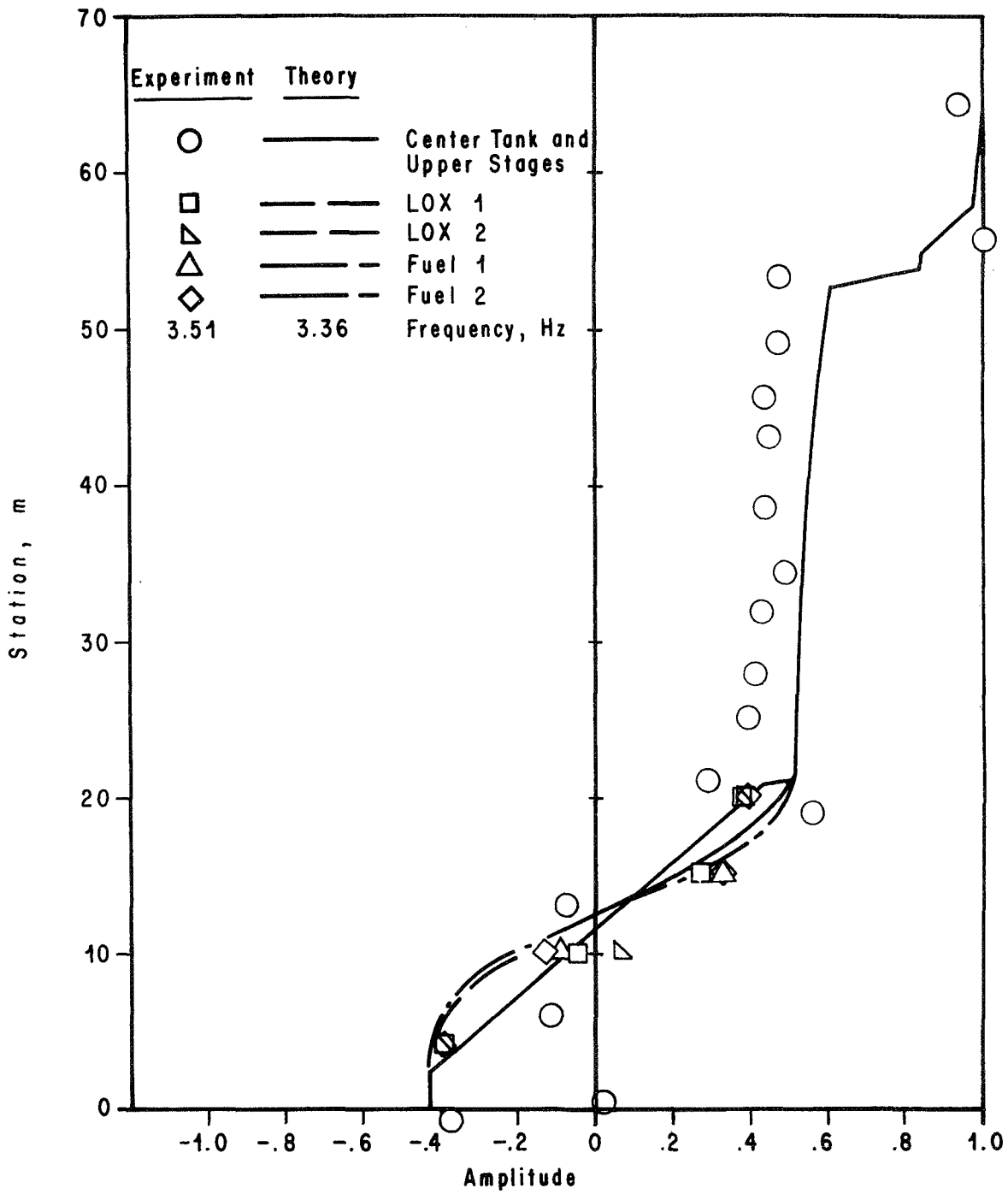


Figure 3. First torsional mode at lift-off.

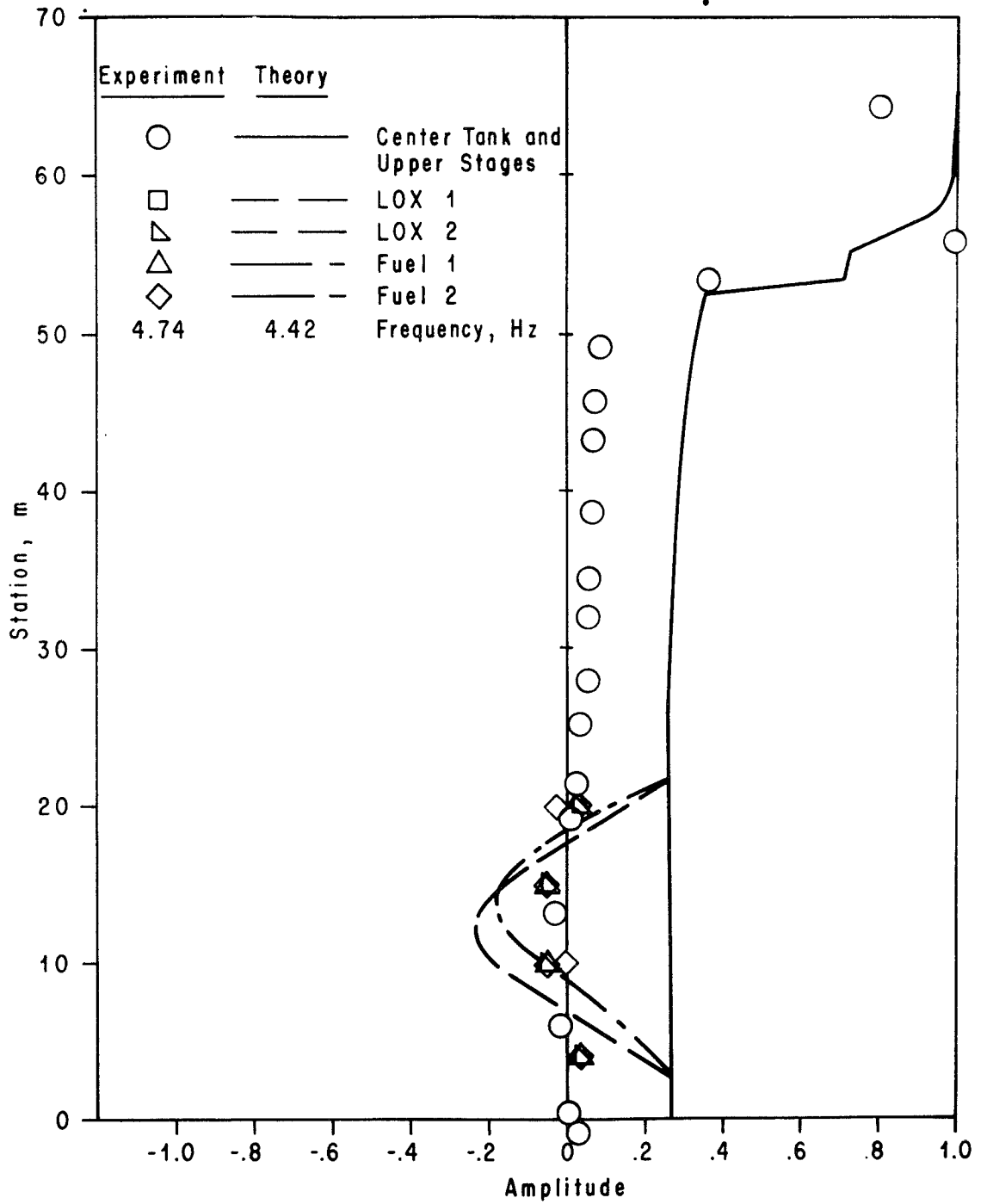


Figure 4. Command module mode at lift-off.

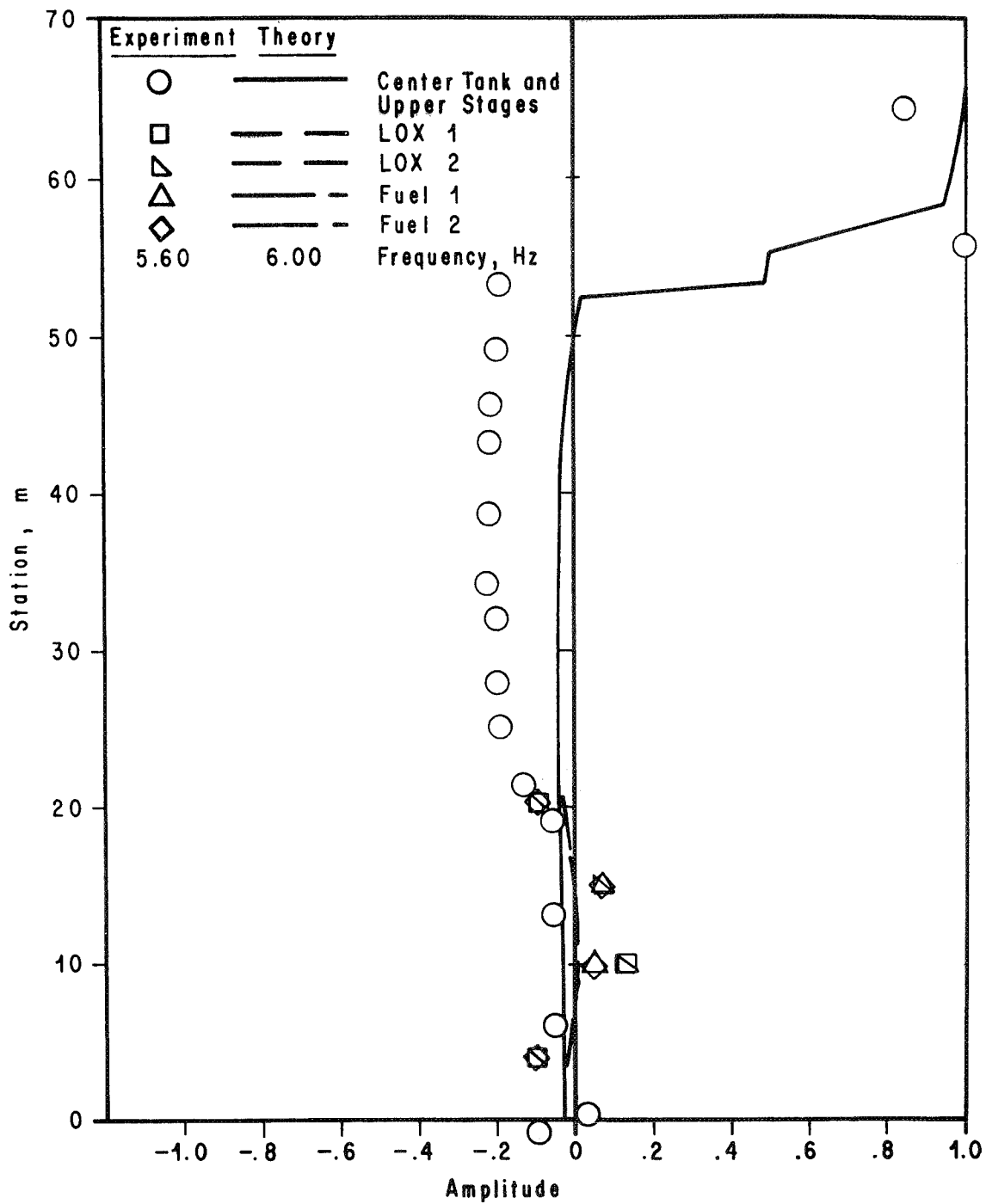


Figure 5. Command module with center body mode at lift-off.

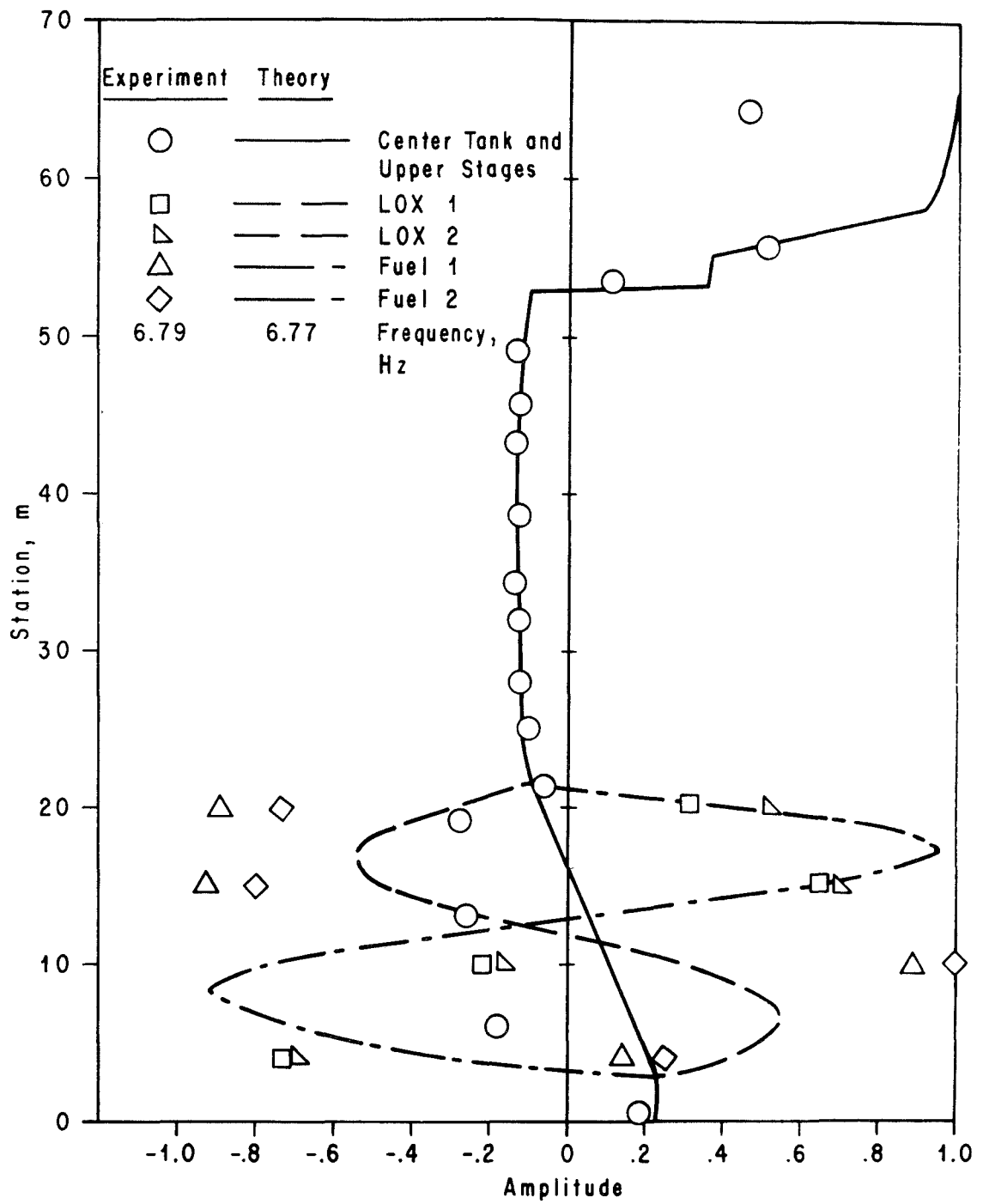


Figure 6. Second outer tank mode at lift-off.

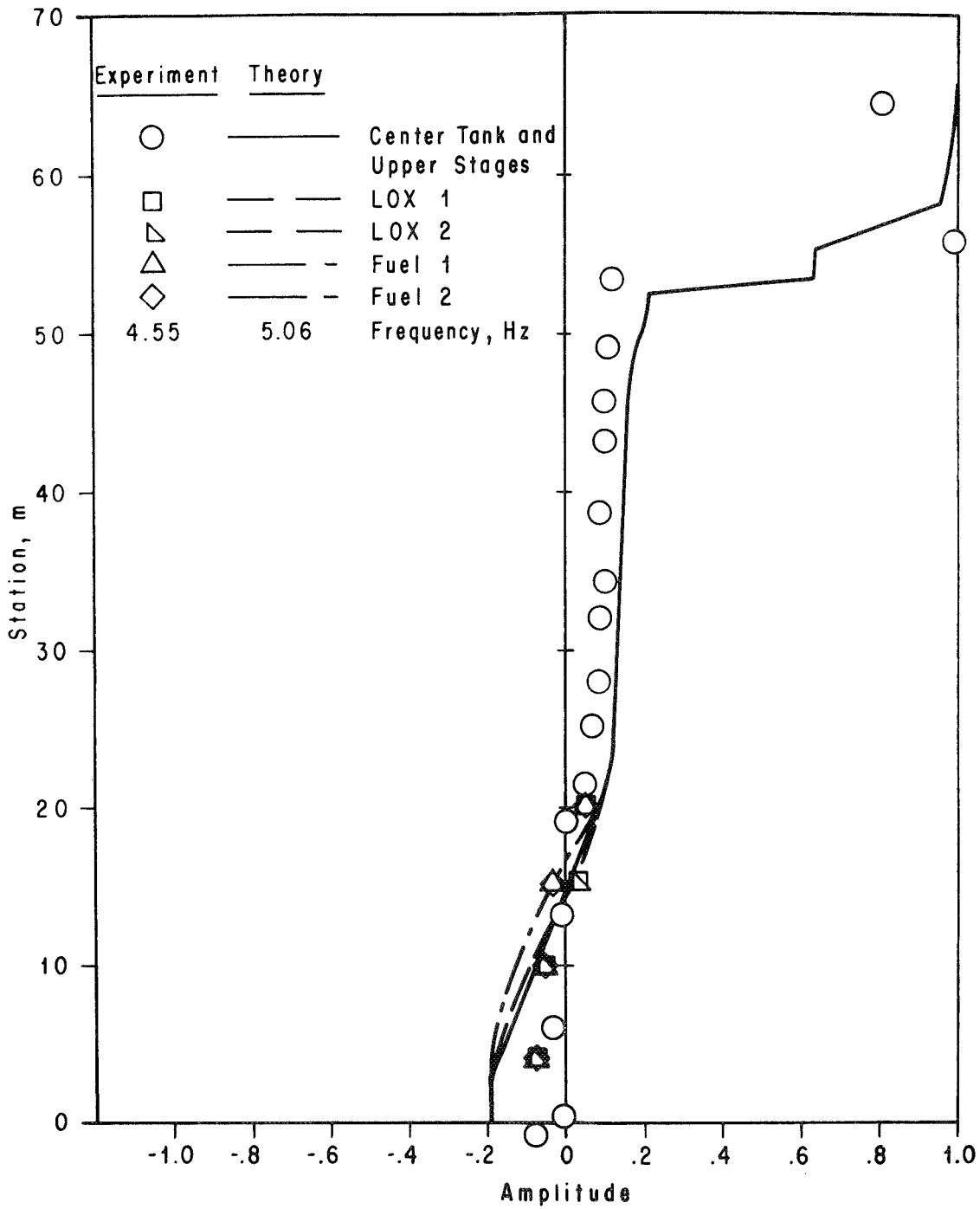


Figure 7. First torsional mode at cut-off.

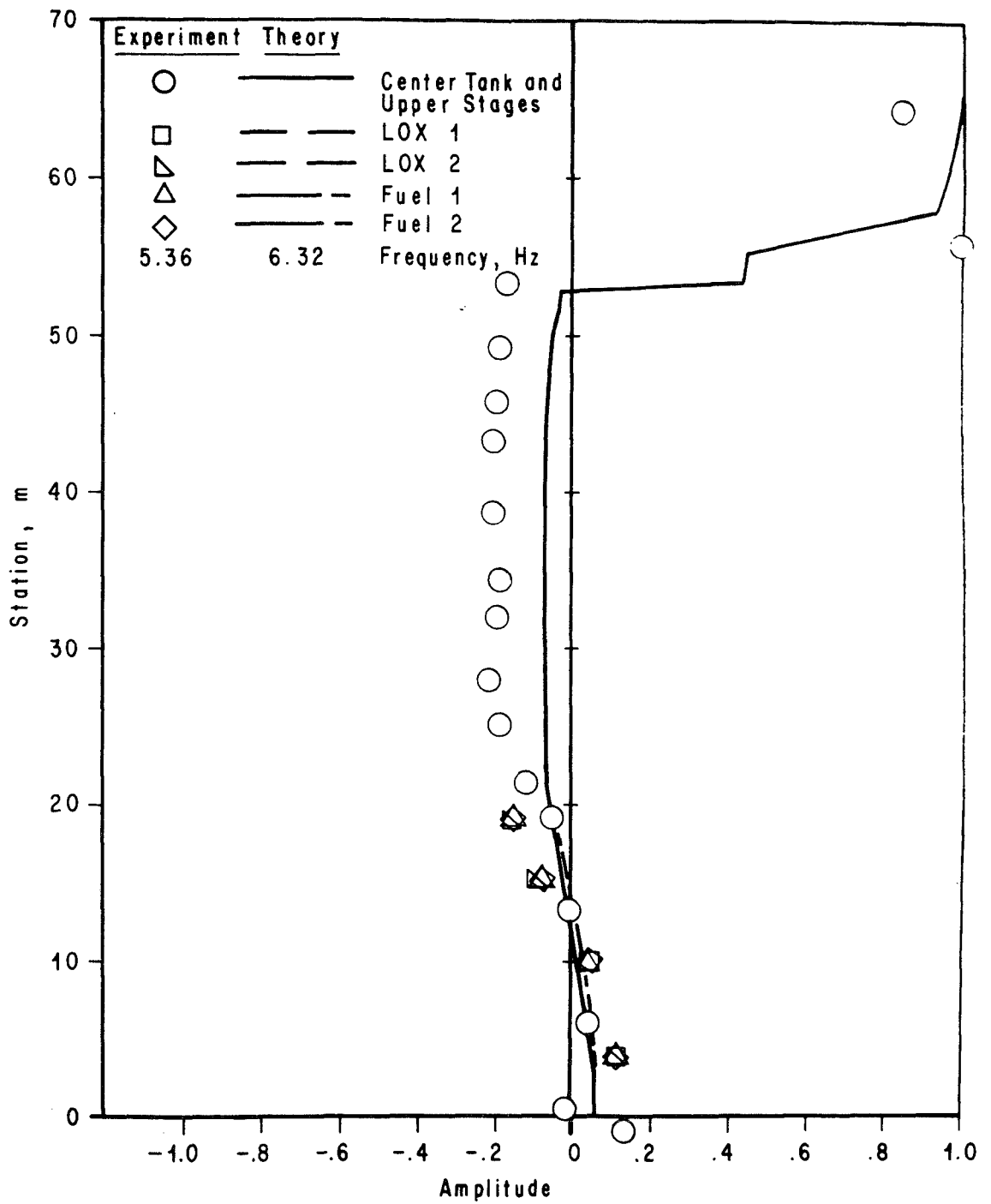


Figure 8. Command module mode at cut-off.

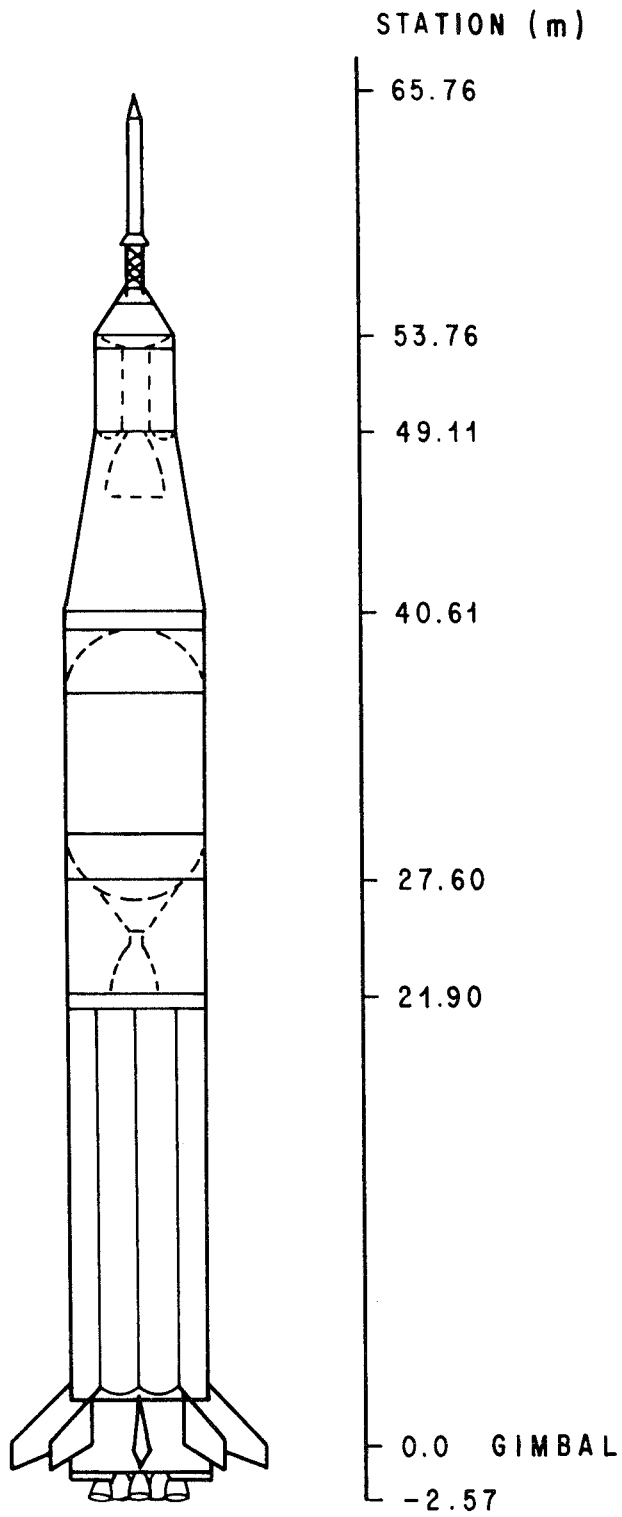


Figure 9. Saturn IB SA-202 configuration.

REFERENCES

1. Kiefling, Larry: Multiple Beam Vibration Analysis of Saturn I and IB Vehicles. NASA TM X-53072, June 24, 1964.
2. Milner, James L. : Three-Dimensional Multiple Beam Analysis of a Saturn I Vehicle. NASA TM X-53098, July 16, 1964.
3. Kiefling, Larry: Modified Stodola Method for Bending Vibration Analysis. R-AERO-IN-22-64, Marshall Space Flight Center, September 18, 1964. (Available from author, S&E-AERO-DDS, George C. Marshall Space Flight Center, Marshall Space Flight Center, Alabama 35812).
4. Final Report of Total Vehicle Testing of Saturn IB Dynamic Test Vehicle, SA-200-D, in SA-202, SA-203, SA-206, SA-207 Configurations. HSM-R856, Space Division, Chrysler Corp. , Huntsville Operations, January 31, 1966.
5. Dynamic Test Results of SAD-202, Technical Report HSM-R148, Space Division, Chrysler Corp. , Huntsville Operations, December 27, 1965.

APPROVAL

TM X-53990

TORSIONAL VIBRATION ANALYSIS OF SATURN VEHICLES


By Larry Kiefling and Frank Bugg

The information in this report has been reviewed for security classification. Review of any information concerning Department of Defense or Atomic Energy Commission programs has been made by the MSFC Security Classification Officer. This report, in its entirety, has been determined to be unclassified.

This document has also been reviewed and approved for technical accuracy.



J. LOVINGOOD
Chief, Dynamics and Control Division



E. D. GEISSLER
Director, Aero-Astroynamics Laboratory

DISTRIBUTION

TM X-53990

INTERNAL

DIR

DEP-T

S&E-ASTN-DIR

Mr. Heimburg

S&E-ASTN-A

Mr. Sterett

S&E-ASTR-DIR

Mr. Moore

S&E-ASTR-F

Mr. Mink

Mr. Guynes

Mr. Darden

S&E-CSE-I

Mr. Blackstone

S&E-AERO-M

Mr. Lindberg

Mr. Moore

S&E-AERO-P

Mr. Sims

Mr. Jackson

S&E-AERO-DO

Mr. Rheinfurth

S&E-AERO-DIR

Dr. Geissler

Mr. Horn

S&E-AERO-D

Dr. Lovingood

Mr. Ryan

S&E-AERO-DDS

Mr. Kiefling

Mr. Bugg (10)

AD-S

A&TS-PAT

Mr. L. D. Wofford, Jr.

PM-PR-M

A&TS-MS-H

A&TS-MS-IP (2)

A&TS-MS-IL (8)

A&TS-TU (6)

EXTERNAL

Scientific and Technical Information

Facility (25)

P. O. Box 33

College Park, Maryland 20740

Attn: NASA Representative (S-AK/RKT)